

Acknowledgment. We thank the National Science Foundation for support of this research. W.T.B. also thanks the National Science Foundation for providing funds that enabled the purchase of the Convex C-2 computer, on which some of the calculations reported here were performed, and the San Diego Supercomputer Center for a generous allocation of time on the Cray Y-MP8/864 computer at SDSC.

Supplementary Material Available: RHF, TCSCF, and ROHF/6-31G* energies used to calculate the hydrogenation energies, π BDEs, and singlet-triplet energy differences reported in the text and complete spectral and analytical data on **4**, **5**, **7**, and the Diels-Alder adduct of **2** with DPIBF (5 pages). Ordering information is given on any current masthead page.

Mobility-Ordered Two-Dimensional Nuclear Magnetic Resonance Spectroscopy

Kevin F. Morris and Charles S. Johnson, Jr.*

Department of Chemistry, University of North Carolina
Chapel Hill, North Carolina 27599-3290

Received September 9, 1991

Recent advances in high-resolution electrophoretic NMR (ENMR) permit the resolution of NMR spectra of mixtures on the basis of electrophoretic mobilities of contributing ions.^{1,2} However, these experiments observe a counterflow of ions and only the magnitudes of the mobilities can be detected. Also, for monodisperse ions, resolution is severely limited by truncation errors in the Fourier transformations with respect to the electric current amplitudes. Here we report an experiment that recovers the signs of mobilities through the use of a cylindrical electrophoresis chamber with appropriate modifications in pulse sequences and data handling. The truncation problem has been solved by means of linear prediction (LP) methods. We note that this experiment determines the electrophoretic mobilities of ions and identifies the ions by their NMR spectra. Furthermore, it does not require labeling of ions for detection, and it permits the use of short (<1-s) migration times.

Our 2D-ENMR experiments are usually performed with the LED pulse sequence shown in Figure 1a.³ This is a stimulated echo (STE) experiment^{4,5} in which two additional $\pi/2$ rf pulses are used to store and recover the stimulated echo so that magnetic field disturbances associated with the gradient pulse at Δ will have time (T_c) to decay. J -modulation effects can also be avoided since the transverse evolution period ($\tau - \delta$) can be as small as 600 μ s.³ For an ion with diffusion coefficient D and electrophoretic mobility μ , the magnetization immediately after the fifth $\pi/2$ rf pulse has the form

$$M(\Delta + \tau + T_c) = \exp[i\phi(I)]f(\tau, \Delta, T_c) \quad (1)$$

where $\phi(I) = K\mu\Delta I/(\kappa A)$, $f(\tau, \Delta, T_c) = (M_0/2) \exp[-2\tau/T_2 - (\Delta + T_c)/T_1 - DK^2(\Delta - \delta/3)]$, $K = \gamma g\delta$, γ is the magnetogyric ratio, and g and δ are the amplitude and duration of the magnetic field gradient pulses, respectively. The electric current I in the sample is given by $I = \kappa AE_{dc}$ where E_{dc} is the electric field, κ is the conductivity, and A is the cross-sectional area of the sample tube. 2D-ENMR spectra are usually obtained by a Fourier transformation with respect to the acquisition time t_2 and a transformation with respect to the current I .

* Author to whom correspondence should be addressed.

(1) Johnson, C. S., Jr.; He, Q. In *Advances in Magnetic Resonance*; Warren, W. S.; Ed.; Academic Press: San Diego, 1989; Vol. 13, p 131.
(2) He, Q.; Hinton, D. P.; Johnson, C. S., Jr. *J. Magn. Reson.* **1991**, *91*, 654.

(3) Gibbs, S. J.; Johnson, C. S., Jr. *J. Magn. Reson.* **1991**, *93*, 395.

(4) Hahn, E. L. *Phys. Rev.* **1950**, *80*, 580.

(5) He, Q.; Johnson, C. S., Jr. *J. Magn. Reson.* **1989**, *85*, 181.

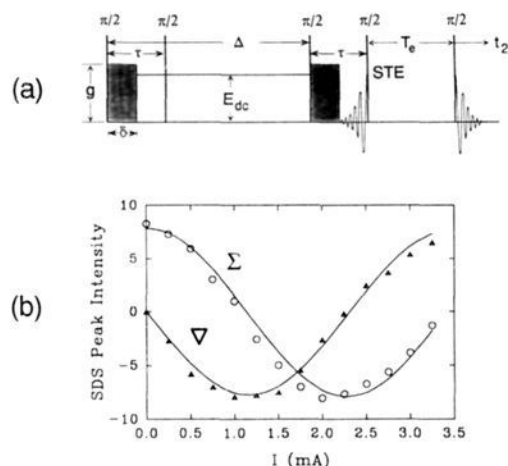


Figure 1. (a) The LED-ENMR pulse sequence. The gradient prepulses, homospoil pulses, and phases of the rf pulses are not shown. (b) A plot of Σ and ∇ for the SDS ^1H peak at 1.08 ppm (see text).

The electrodes must be arranged so that bubbles can escape. U-tube chambers satisfy this condition but yield low filling factors for receiver coils, difficult shimming for the magnetic field, spectral phasing problems, and a counterflow of ions. Since there are equal contributions from ions having positive and negative velocities, the phase factor in eq 1 must be replaced with $\cos [K\mu\Delta I/(\kappa A)]$ and information about the sign of the electrophoretic mobility is lost. As an alternative we have developed a chamber made up of two concentric tubes. The outer tube (10.0 mm o.d.) is sealed at the bottom, and the inner tube (3–5 mm o.d.) is open at both ends. The inner tube is held in place by a 1.0-cm-long Teflon spacer at the top and contains a 4-mm polyacrylamide gel plug at the bottom to separate the two chambers. A salt solution fills the annulus between the tubes, and the solution under study fills the inner tube. This arrangement, which permits Pt electrodes to be placed in the top of both chambers, is practical for commercial NMR probes.

When the STE version of the experiment is adequate, the last two rf pulses in Figure 1a are deleted and the acquired FID is just the second half of the stimulated echo. The reverse precession method can then be used to determine the sign of the mobility.⁶ For each value of the current, FIDs are collected with positive and negative polarities of the electric field. After Fourier transformation with respect to t_2 , the signals with positive and negative polarities can be represented by

$$S_{\pm}(\omega_2, I) = S_0 \exp[\pm i\phi(I)]f(\tau, \Delta, T_c)[a(\omega_2) + id(\omega_2)] \quad (2)$$

where $a(\omega_2)$ and $d(\omega_2)$ are Lorentzian absorption and dispersion components.⁷ The combinations $\Sigma = \text{Re}(S_+ + S_-)$ and $\nabla = \text{Im}(S_+ - S_-)$ give absorption spectra modulated by $\cos [K\mu\Delta I/(\kappa A)]$ and $\sin [K\mu\Delta I/(\kappa A)]$, respectively. These data sets can be analyzed to obtain the magnitude and sign of μ or transformed with respect to current to obtain a 2D-ENMR spectrum with positive and negative mobility values.

When the full LED sequence is used, the fourth $\pi/2$ pulse is directed along the $-x$ and $-y$ directions in the rotating frame in order to store the real and imaginary parts of the magnetization, respectively. Typically the polarity of the electric field is negative when the real component is stored and positive when the imaginary part is stored. This yields the correct signs for the mobilities and prevents mass polarization of the sample. Figure 1b shows LED-ENMR data for an anion in an aqueous solution containing 2.0 mM tetramethylammonium chloride (TMA) and 2.0 mM sodium dodecyl sulfate (SDS) stabilized by 0.5% agarose gel. The

(6) Bachmann, P.; Aue, W. P.; Müller, L.; Ernst, R. R. *J. Magn. Reson.* **1977**, *28*, 29.

(7) Ernst, R. R.; Bodenhausen, G.; Wokaun, A. *Principles of Nuclear Magnetic Resonance in One and Two Dimensions*; Clarendon Press: Oxford, 1987; p 309.

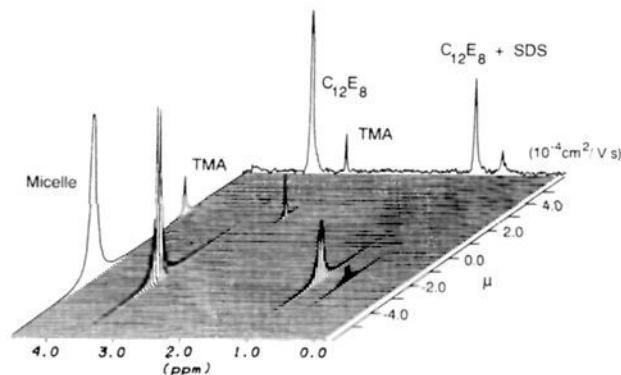


Figure 2. The mobility-ordered 2D-NMR spectrum of a sample containing TMA and mixed micelles.

^1H spectra were obtained with a Bruker AC-250 spectrometer with custom-built probe and ENMR electronics as previously described.^{1,8,9} The parameters were $K = 770\text{ cm}^{-1}$, $\Delta = 0.500\text{ s}$, $T_c = 25.0\text{ ms}$, $A = 0.0820\text{ cm}^2$, and $\kappa = 0.320\text{ mS}\cdot\text{cm}^{-1}$. The ∇ values in Figure 1b for SDS protons show that the mobility is negative.

Figure 2 displays the complete mobility-ordered spectrum (MOSY) for a sample containing TMA (2.00 mM) with mixed micelles (1.50 mM SDS and 4.00 mM octaethylene glycol dodecyl ether (C_{12}E_8)). The data were obtained in an STE-ENMR experiment with $K = 722\text{ cm}^{-1}$, $\Delta = 0.400\text{ s}$, $T_c = 25.0\text{ ms}$, $A = 0.0986\text{ cm}^2$, and $\kappa = 0.273\text{ mS}\cdot\text{cm}^{-1}$. Data collection was limited to currents below 0.75 mA because of heating effects at higher currents. In this current range the HOD signal (not shown) was constant and confirmed the absence of electroosmosis and convection. The severely truncated data sets were successfully transformed by means of the linear prediction (LPZOOM) procedure,¹⁰ but other analysis schemes for limited data sets could have been used. The mobilities obtained from the peak maxima reported by LPZOOM are 2.75×10^{-4} and $-1.55 \times 10^{-4}\text{ cm}^2\cdot\text{V}^{-1}\cdot\text{s}^{-1}$ for protons in TMA and micelles, respectively. It should be noted that the peak at 3.51 ppm is entirely associated with C_{12}E_8 and its position on the mobility axis indicates that this neutral compound is migrating with the micelle. Also, the mobility of the TMA cation in the mixture is less than the value of $3.60 \times 10^{-4}\text{ cm}^2\cdot\text{V}^{-1}\cdot\text{s}^{-1}$ reported for TMA alone in aqueous solution¹¹ and suggests a possible interaction between the anionic micelle and $(\text{Me})_4\text{N}^+$. This is a topic for future study. Figure 2 clearly shows the range and resolution of mobilities that are now accessible in 2D-ENMR.

We conclude with comments about the line widths. Since the migration time Δ is held constant, there can be no diffusional broadening in the mobility dimension; however, the intensities depend on the diffusion coefficients as indicated in eq 1. Polydispersity, of course, leads to damped oscillations of intensity versus current and thus to line broadening, and in favorable cases the interferograms can be transformed to obtain the mobility distribution function.² However, no damping was evident in the data sets used to generate Figure 2, and the line widths resulted from intensity noise and the LPZOOM procedure. The line widths in the chemical shift dimension are consistent with the magnetic field inhomogeneity over the 5-mm nonspinning sample.

Acknowledgment. This work was supported under National Science Foundation Grant CHE-8921144. We thank Prof. J. R. Norris and Dr. J. Tang for providing LPZOOM software and Dr. S. J. Gibbs for help with programming and instrumentation.

(8) Saarinen, T. R.; Woodward, W. S. *Rev. Sci. Instrum.* **1988**, *59*, 761.

(9) Gibbs, S. J.; Morris, K. F.; Johnson, C. S., Jr. *J. Magn. Reson.* **1991**, *94*, 165.

(10) Tang, J.; Norris, J. R. *J. Magn. Reson.* **1988**, *79*, 190.

(11) Saarinen, T. R.; Johnson, C. S., Jr. *J. Am. Chem. Soc.* **1988**, *110*, 3332.

A New Reaction for the Synthesis of Carbene Precursors from Aldehydes and $\text{Cp}(\text{CO})_2\text{Fe}\cdot\text{M}^+$ ($\text{M} = \text{Na, K}$)

Roy M. Vargas, Ronald D. Theys, and M. Mahmud Hossain*

Department of Chemistry
University of Wisconsin—Milwaukee
Milwaukee, Wisconsin 53201

Received January 18, 1991

Electrophilic iron carbene complexes are of interest as highly reactive intermediates for metal-catalyzed cyclopropanation reactions, for which there is considerable potential synthetic utility. Due to lability, these carbene complexes are often generated from their corresponding precursors prior to use. Several techniques have already been devised for the generation of electrophilic iron carbenes from their precursors;¹ however, each has inherent limitations. We report here a simple, efficient strategy for synthesis of electrophilic iron carbene precursors from readily available aldehydes of low toxicity.

The precursors **4** for the electrophilic iron carbene complexes were prepared in very good to moderate yield by the reaction of the Fp anion **1** with aldehydes **2**. The resulting alkoxides **3** were trapped with chlorotrimethylsilane² (Scheme I). In a typical reaction,³ 1.2–4 equiv of aldehyde were added to 1 equiv of the Fp anion in dried and degassed tetrahydrofuran at $-78\text{ }^\circ\text{C}$. The solution was stirred for 1–3 h at $-78\text{ }^\circ\text{C}$, and 1–2 equiv of chlorotrimethylsilane were added dropwise to the solution. The mixture was stirred at $-78\text{ }^\circ\text{C}$ for an additional hour. The crude product was concentrated under vacuum, and elution from a low-temperature silica gel or alumina column with a 5% THF-pentane mixture provided pure (siloxyalkyl)irons **4a,b** as red-brown oils and **4c** as a cream-colored solid. Precursor **4d** was purified by extraction with pentane at $-78\text{ }^\circ\text{C}$ and concentrated under vacuum due to its thermal instability. The precursors **4** were characterized by spectroscopic methods.^{4,5}

The reaction depicted in Scheme I is apparently the first successful nucleophilic addition of a metal anion to an aldehyde.⁶ Gladysz⁷ failed to observe any reaction between the manganese

(1) Previously, the most widely used techniques to synthesize carbene precursors from Fp anion utilized α -chloroalkyl methyl ethers (CICH(R)-OCH_3): (a) Brookhart, M.; Nelson, G. O. *J. Am. Chem. Soc.* **1977**, *99*, 6099. The use of α -chloroalkyl methyl thioethers (CICH(R)SCH_3) to produce considerably more stable precursors was also exhibited. (b) O'Connor, E. J.; Brandt, S.; Helquist, P. *Ibid.* **1987**, *109*, 3739. (c) Kremer, K. A. M.; Helquist, P. *J. Organomet. Chem.* **1985**, *285*, 231. An alternative to the α -ether has been devised involving hydride reduction of a Fischer carbene. (d) Brookhart, M.; Studabaker, W. B. *Chem. Rev.* **1987**, *87*, 411. (e) Casey, C. P.; Miles, W. H. *J. Organomet. Chem.* **1983**, *254*, 333. Another, less frequently used, technique utilizes iron vinyl complex protonation to synthesize iron carbenes. (f) Casey, C. P.; Miles, W. H.; Tukada, H. *J. Am. Chem. Soc.* **1985**, *107*, 2924. (g) Kuo, G. H.; Helquist, P.; Kerber, R. C. *Organometallics* **1984**, *3*, 806. (h) Kremer, K. A. M.; Kuo, G. H.; O'Connor, E. J.; Helquist, P.; Kerber, R. C. *J. Am. Chem. Soc.* **1982**, *104*, 6119. (i) Casey, C. P.; Miles, W. H.; Tukada, H.; O'Connor, J. M. *J. Am. Chem. Soc.* **1982**, *104*, 3761.

(2) Treatment of the alkoxide intermediate with methyl iodide or trimethylxonium tetrafluoroborate generated only the methyl complex $\text{Cp}(\text{CO})_2\text{FeCH}_3$ and Fp dimer. No $\text{FpCH}(\text{OCH}_3)_2$ was formed, indicating that neither CH_3I nor $(\text{CH}_3)_3\text{O}^+\text{BF}_4^-$ was an effective trapping reagent for the alkoxide **3** intermediate.

(3) Details contained in the supplementary material.

(4) See the supplementary material for complete spectral and analytical data.

(5) Cutler has recently published a paper for the synthesis of Fp-(α -siloxyalkyl) complexes as "stable products" from FpCOR complexes by hydrosilylation in the presence of a manganese acetyl catalyst. Hanna, P. K.; Gregg, B. T.; Cutler, A. R. *Organometallics* **1991**, *10*, 31. Similarly, we have found by observation that the siloxy phenyl iron and siloxy *p*-methoxyphenyl iron complexes **4a,c** are stable, allowing acquisition of the CH microanalysis. The siloxy methyl iron complexes **4b,d** are less stable.

(6) Hegedus has reacted $\text{Cr}(\text{CO})_3^{2-}$ with tertiary amides in the presence of chlorotrimethylsilane to produce aminocarbene complexes through $(\text{CO})_3\text{Cr}(\text{NR}'_2\text{CRO})$. This reaction is restricted to tertiary amides. See: Imwinkelried, R.; Hegedus, L. S. *Organometallics* **1988**, *7*, 702.

(7) Gladysz, J. A.; Selover, J. C.; Strouse, C. E. *J. Am. Chem. Soc.* **1978**, *100*, 6766.